



OPEN

DATA DESCRIPTOR

A Time-of-Flight and Radar Dataset of a neonatal Thorax Simulator with synchronized Reference Sensor Signals for respiratory Rate Detection

Johanna Gleichauf¹✉, Sven Herrmann¹, Christine Niebler¹ & Alexander Koelpin²

In this paper we present an open-source Time-of-Flight and radar dataset of a neonatal thorax simulator for the development of respiratory rate detection algorithms. As it is very difficult to gain recordings of (preterm) neonates and there is hardly any open-source data available, we built our own neonatal thorax simulator which simulates the movement of the thorax due to respiration. We recorded Time-of-Flight (ToF) and radar data at different respiratory rates in a range of 5 to 80 breaths per minute (BPM) and with varying upstroke heights. As gold standard a laser micrometer was used. The open-source data can be used to test new algorithms for non-contact respiratory rate detection.

Background & Summary

Preterm neonates require continuous monitoring of their vital parameters. The current monitoring methods (e.g. ECG, pulse oximetry, etc.) have in common that they require direct contact to the neonate's sensitive skin. This can lead to skin irritations, pressure marks, eczema and even the removal of the skin. To reduce these risks non-contact monitoring methods are being developed. To develop such algorithms data for testing and validation is required. To gain real data is expensive and difficult due to ethical and regulatory restrictions. There exist no open-source datasets as this data is medical patient data. In order to develop non-contact respiratory rate detection algorithms based on ToF and radar data, a neonatal thorax simulator was designed in previous work which simulates the thorax movement due to respiration¹. We recorded datasets of 15 minutes at different respiratory rates (5, 10, 20, 30, 40, 45, 50, 55, 60 and 80 BPM) and in different modes (*normal* and *deep*).

Methods

In this section we describe the concept behind our neonatal thorax simulator as well as all used sensors for the recording of this dataset. The recordings were part of our previous work¹. The recording setup is shown in Fig. 1. We will now describe each part in detail.

Neonatal thorax simulator. Our neonatal thorax simulator simulates the thorax movement due to respiration and is made up of a speaker (by company Visaton (<https://www.conrad.de/de/p/visaton-fr-10-4-zoll-10-16-cm-breitband-lautsprecher-chassis-20-w-4-303634.html>)), an amplifier circuit (by company Conrad (<https://www.conrad.de/de/p/conrad-components-stereo-verstaerker-bausatz-9-v-dc-12-v-dc-18-v-dc-35-w-2-1216582.html>)) and a computer. The generation of the respiratory signals is done by a software program on the computer. Our idea was to superimpose two sine waves: one for the respiration and a decaying sine for the heartbeat for future developments. We are aware that real breathing patterns are more complex than a sinusoidal signal which would require the

¹Nuremberg Institute of Technology, Department of Electrical Engineering, Precision Engineering and Information Technology, Nuremberg, 90489, Germany. ²Hamburg University of Technology, Institute of High-Frequency Technology, Hamburg, 21073, Germany. ✉e-mail: johanna.gleichauf@th-nuernberg.de

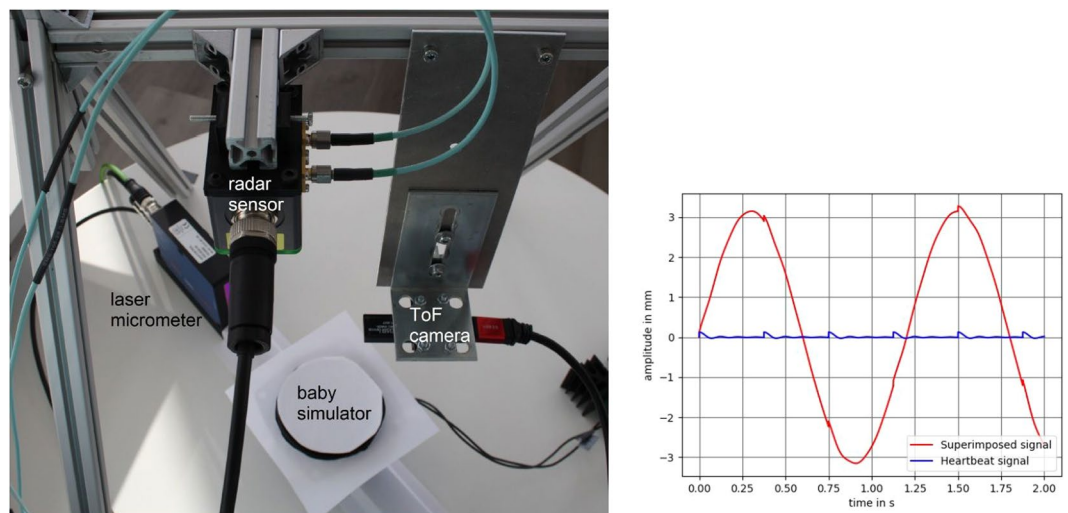


Fig. 1 Hardware setup for the ToF-radar system (left). The neonatal thorax simulator can be seen in the middle, and the laser micrometer serves as reference measurement¹. On the right the simulated signal can be seen.

| BPM | Interbeat interval | Stroke in mm | |
|-----|--------------------|--------------|-------------|
| | | deep mode | normal mode |
| 5 | 12 s | 0.305 | 0.136 |
| 10 | 6 s | 0.644 | 0.273 |
| 20 | 3 s | 1.344 | 0.589 |
| 30 | 2 s | 1.965 | 0.928 |
| 40 | 1.5 s | 2.591 | 1.285 |
| 45 | 1.33 s | 2.797 | 1.394 |
| 50 | 1.2 s | 3.047 | 1.66 |
| 55 | 1.09 s | 3.285 | 1.72 |
| 60 | 1 s | 3.472 | 1.917 |
| 80 | 0.75 s | 4.068 | 2.481 |

Table 1. Measured strokes with the laser micrometer in *deep* and *normal* mode¹.

time for breathing in and out as well as holding the breath to be set. Unfortunately, the amplifier used for our system is incapable of passing low frequency signals, which would be necessary for generating the plateau part of the pattern. Furthermore, the speaker would not cope with the DC-signals. Therefore, we use the simplified sine signal as for now.

The resulting signal (see Fig. 1) is then transmitted from the AUX output of the computer to the speaker via the amplifier circuit. Due to the small output power of the computer, the amplifier was required to reach the desired amplitude in the speaker's membrane displacement. The electrical signal is then transformed into the movement of the speaker membrane.

The simulator has two respiratory simulation modes: *normal* and *deep*, with *deep* mode providing strokes of twice the size than *normal* mode. The exact stroke sizes can be found in Table 1.

The code for generating the signals to be simulated by the speaker can be found within our figshare repository².

Time-of-Flight camera. The 3D Time-of-Flight camera uses the phase difference method for calculating the distance to objects (<https://pmdtec.com/picofamily/faq/>). The distance is determined using the phase shift ϕ and the wavelength λ of the reflected modulated signal:

$$d = \frac{\phi}{2 \cdot \pi} \cdot \frac{\lambda}{2} \quad (1)$$

The 3D imager detects the infrared light reflection and then uses the phase shift for calculating the distance to the object. This results in a 3D point cloud.

We used the CamBoard pico flexx 3D time-of-flight camera by the company pmd (see Fig. 2). The measurement range lies between 0.1–4m. The camera has a field of view (FoV) of $62^\circ \times 45^\circ$ and a resolution of 224×171 (38k) pixels. A frame rate of up to 45 fps (3D frames) can be selected. For using the camera an Ubuntu 16.04 computer with Robot Operating System (ROS) Kinetic installed is required. The driver used is the Royale SDK

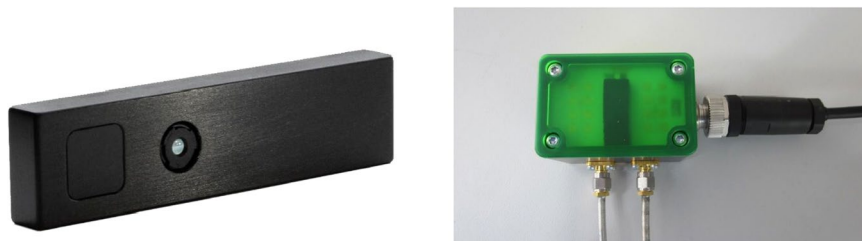


Fig. 2 Pico flexx 3D time-of-flight camera by pmd (https://pmdtec.com/picofamily/wp-content/uploads/2018/03/PMD_DevKit_Brief_CB_pico_flexx_CE_V0218-1.pdf) (left) and radar sensor by InnoSenT (right)¹.

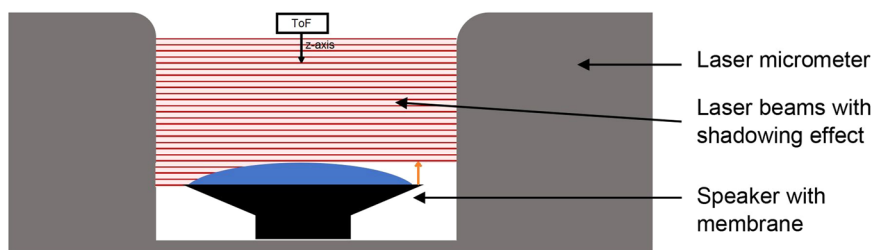


Fig. 3 Hardware setup of the neonatal thorax simulator. The speaker membrane changes its upstroke size. We are only interested in the change of height which is detected by the light curtain (see orange arrow)¹.

provided by pmd as well as the ROS package *pico_flexx_driver* (https://github.com/code-iai/pico_flexx_driver). We set the frame rate to 35 fps as this is a frame rate commonly used for cameras in this context.

Radar sensor. The radar sensor we used is a microwave interferometric radar sensor based on Continuous Wave (CW) radar. One characteristic of this sensor is that no Fourier transform is needed and only the phase shift between the reflected and the reference microwave has to be determined. The relative distance is calculated using the following formula:

$$\Delta x = \frac{\Delta \sigma}{2 \cdot \pi} \cdot \frac{\lambda}{2} \quad (2)$$

with Δx as relative distance, $\Delta \sigma$ as relative phase shift and λ as wavelength. The relative phase shift can also be represented by its In-Phase (I) and Quadrature (Q) signal:

$$\Delta \sigma = \arctan \frac{I}{Q} \quad (3)$$

We chose the microwave interferometric radar sensor iSYS-4001 by the company InnoSenT (see Fig. 2). The radar sensor was originally designed for the research project GUARDIAN (<https://www.technik-zum-menschen-bringen.de/projekte/guardian>), which is applied for the monitoring of vital parameters of patients in the palliative care unit. The frequency of the radar sensor lies at 24.2 GHz and it has a power of 100 mW (20dBm) which lies within the legally approved norm range. An Infineon XMC4500 microcontroller receives and transfers the radar signal. The raw data (In-Phase (I) and Quadrature (Q) signal) is digitized by an analog-to-digital converter (ADC), ADS1298 by Texas Instruments, due to its higher performance than the inbuilt ADC of the Infineon XMC4500 microcontroller. This is done with a sampling rate of 2 kHz. The digitized data is then sent via Ethernet to the computer.

Reference laser micrometer. As gold standard a precise reference measurement has to be used. This sensor needs to have the following characteristics: it has to be able to detect small movements such as the displacement of the thorax even due to the heartbeat (for future work), which lie within the submillimeter range. A laser micrometer based on the principle of shadowing is a good choice (<https://www.micro-epsilon.co.uk/service/glossar/optoCONTROL.html>, <https://www.micro-epsilon.co.uk/download/manuals/man-optoCONTROL-2520-en.pdf>). When an object moves into the light carpet, a change can be sensed (see Fig. 3).

We used the optoCONTROL 2520 laser micrometer by MICRO-EPSILON (https://www.micro-epsilon.co.uk/2D_3D/optical-micrometer/micrometer/optoCONTROL_2520/). The maximum resolution is 1 μ m and has a measurement range of 46 mm. The inbuilt laser is of laser class 1M, such that no harm is applied to the user. But it should not be magnified by any optical instrument. The laser micrometer's receiver and transmitter are connected via a CE2520-1 cable. A 24 V power supply is needed. For starting the measurement the optoCONTROL is connected to a Microsoft Windows 10 laptop via Ethernet. The manufacturer delivers a measurement

| Name | BPM | Mode | Modality | Filename |
|--------------|-----|--------|----------|----------------------------|
| 05BPM_normal | 5 | normal | radar | iq_values_05BPM_normal.csv |
| | | | ToF | ToF_05BPM_normal |
| | | | laser | laser_05BPM_normal.csv |
| 05BPM_deep | 5 | deep | radar | iq_values_05BPM_deep.csv |
| | | | ToF | ToF_05BPM_deep |
| | | | laser | laser_05BPM_deep.csv |
| 10BPM_normal | 10 | normal | radar | iq_values_10BPM_normal.csv |
| | | | ToF | ToF_10BPM_normal |
| | | | laser | laser_10BPM_normal.csv |
| 10BPM_deep | 10 | deep | radar | iq_values_10BPM_deep.csv |
| | | | ToF | ToF_10BPM_deep |
| | | | laser | laser_10BPM_deep.csv |
| 20BPM_normal | 20 | normal | radar | iq_values_20BPM_normal.csv |
| | | | ToF | ToF_20BPM_normal |
| | | | laser | laser_20BPM_normal.csv |
| 20BPM_deep | 20 | deep | radar | iq_values_20BPM_deep.csv |
| | | | ToF | ToF_20BPM_deep |
| | | | laser | laser_20BPM_deep.csv |
| 30BPM_normal | 30 | normal | radar | iq_values_30BPM_normal.csv |
| | | | ToF | ToF_30BPM_normal |
| | | | laser | laser_30BPM_normal.csv |
| 30BPM_deep | 30 | deep | radar | iq_values_30BPM_deep.csv |
| | | | ToF | ToF_30BPM_deep |
| | | | laser | laser_30BPM_deep.csv |
| 40BPM_normal | 40 | normal | radar | iq_values_40BPM_normal.csv |
| | | | ToF | ToF_40BPM_normal |
| | | | laser | laser_40BPM_normal.csv |
| 40BPM_deep | 40 | deep | radar | iq_values_40BPM_deep.csv |
| | | | ToF | ToF_40BPM_deep |
| | | | laser | laser_40BPM_deep.csv |

Table 2. Overview datasets 5–40 BPM.

tool called ODC2520 DAQ tool, which was installed. The tool automatically searches for a laser micrometer and connects to it. For our purpose, the mode “Edge light-dark” needs to be selected within its web interface.

Data Records

Our herein published dataset contains radar, ToF, and laser micrometer reference data. The data was recorded for the following respiratory rates within *deep* and *normal* mode: 5, 10, 20, 30, 40, 45, 50, 55, 60 and 80 BPM. For the radar sensor the IQ values are saved within a csv file with the corresponding timestamps. The ToF pointcloud measurements were saved as png images such that the z-value was saved at the correct coordinate value of the image. The timestamps are found within the png image name. The laser micrometer delivers height values which are saved with the corresponding timestamps within csv files. An overview over all files can be found within Tables 2 and 3. For those interested in our algorithm results, please refer to our results within our previous work¹.

The dataset is available within the following figshare repository².

Technical Validation

In order to ensure a high quality dataset, first of all the correctness of the laser micrometer measurements had to be confirmed. The set BPM from the simulator were compared with the BPM measured with the laser micrometer by manually counting the peaks. Following, the laser micrometer was used as reference for the ToF camera and radar data. Before comparing the distance measurements several signal processing steps had to take place to receive the distance signal from the camera and the radar sensor. These can be found in Figs 4 and 5 displaying the flowchart. The marked component shows the distance we are using for comparison.

Figure 6 shows the synchronized distance signals at 45 BPM. At the beginning a synchronization signal can be observed. All signals are in sync. The amplitude of the ToF signal is very similar to the laser micrometer signal. The radar amplitude differs due to Ellipse fitting. Further information on this phenomenon can be found in¹.

As the time domain signals in Fig. 6 show a good correspondence, we believe the same will be given in case of a more realistic non-sinusoidal signal with plateaus, as the here used DC-coupled interferometric radar sensor as well as the ToF camera are very sensitive in measuring static positions.

| Name | BPM | Mode | Modality | Filename |
|--------------|-----|--------|----------|----------------------------|
| 45BPM_normal | 45 | normal | radar | iq_values_45BPM_normal.csv |
| | | | ToF | ToF_45BPM_normal |
| | | | laser | laser_45BPM_normal.csv |
| 45BPM_deep | 45 | deep | radar | iq_values_45BPM_deep.csv |
| | | | ToF | ToF_45BPM_deep |
| | | | laser | laser_45BPM_deep.csv |
| 50BPM_normal | 50 | normal | radar | iq_values_50BPM_normal.csv |
| | | | ToF | ToF_50BPM_normal |
| | | | laser | laser_50BPM_normal.csv |
| 50BPM_deep | 50 | deep | radar | iq_values_50BPM_deep.csv |
| | | | ToF | ToF_50BPM_deep |
| | | | laser | laser_50BPM_deep.csv |
| 55BPM_normal | 55 | normal | radar | iq_values_55BPM_normal.csv |
| | | | ToF | ToF_55BPM_normal |
| | | | laser | laser_55BPM_normal.csv |
| 55BPM_deep | 55 | deep | radar | iq_values_55BPM_deep.csv |
| | | | ToF | ToF_55BPM_deep |
| | | | laser | laser_55BPM_deep.csv |
| 60BPM_normal | 60 | normal | radar | iq_values_60BPM_normal.csv |
| | | | ToF | ToF_60BPM_normal |
| | | | laser | laser_60BPM_normal.csv |
| 60BPM_deep | 60 | deep | radar | iq_values_60BPM_deep.csv |
| | | | ToF | ToF_60BPM_deep |
| | | | laser | laser_60BPM_deep.csv |
| 80BPM_normal | 80 | normal | radar | iq_values_80BPM_normal.csv |
| | | | ToF | ToF_80BPM_normal |
| | | | laser | laser_80BPM_normal.csv |
| 80BPM_deep | 80 | deep | radar | iq_values_80BPM_deep.csv |
| | | | ToF | ToF_80BPM_deep |
| | | | laser | laser_80BPM_deep.csv |

Table 3. Overview datasets 45–80 BPM.

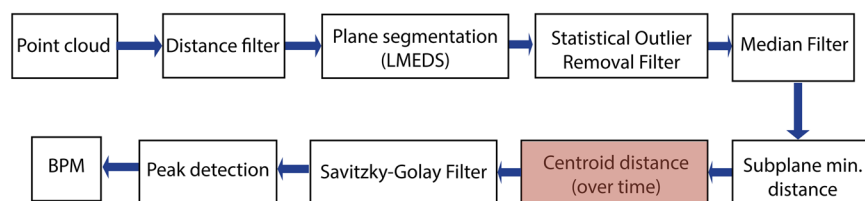


Fig. 4 ToF signal processing flow chart to generate the distance signal¹.

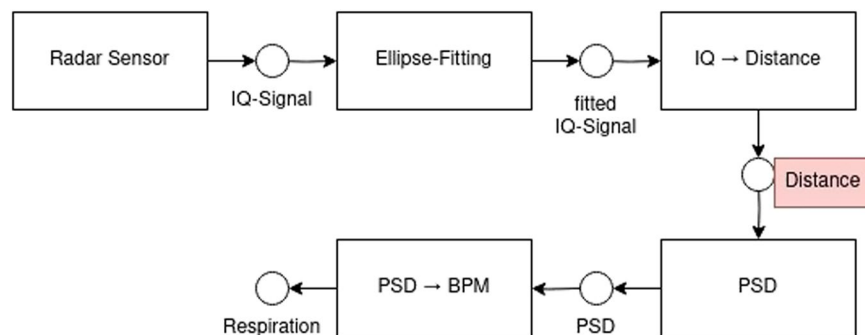


Fig. 5 Radar signal processing flow chart to generate the distance signal.

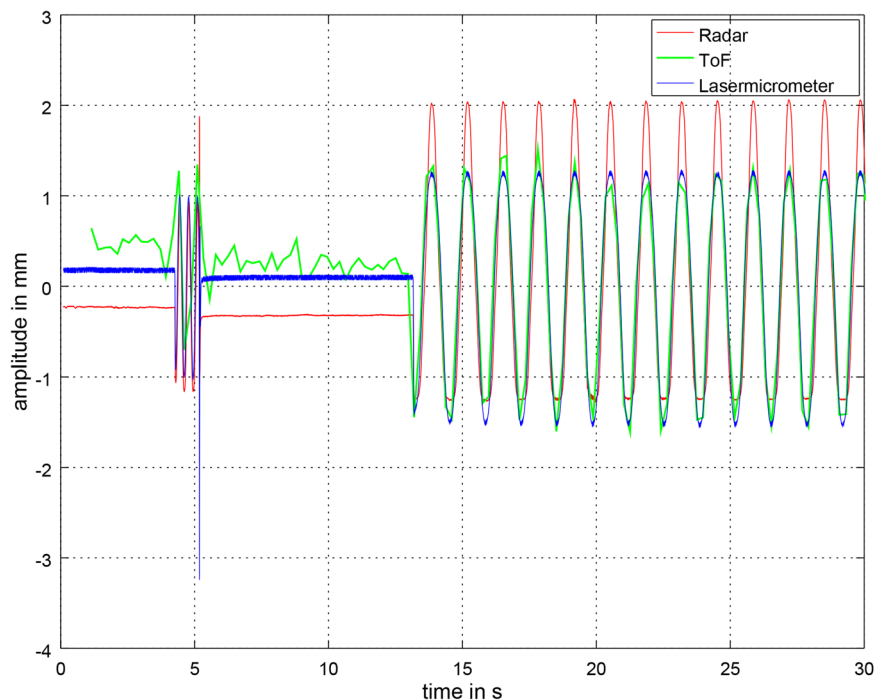


Fig. 6 The figure shows the synchronized distance signals at 45 BPM. At the beginning a synchronization signal can be observed. All signals are in sync. The amplitude of the ToF signal is very similar to the laser micrometer signal. The radar amplitude differs due to Ellipse fitting. Further information on this phenomenon can be found in¹.

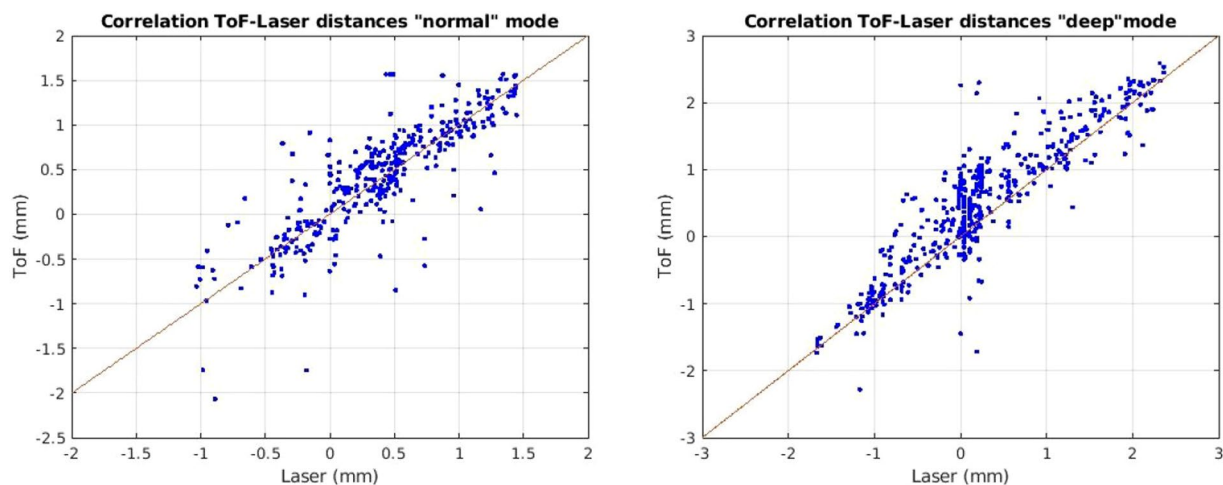


Fig. 7 Correlation between laser and ToF distance signal for *normal* (le.) and *deep* (ri.) mode.

In Figure 7 the correlation between the distance signal of the ToF camera and the laser micrometer can be found. As can be seen the overall precision is high. Inaccuracies are due to the low signal-to-noise ratio at low frequencies such as 5 and 10 BPM.

In Fig. 8 the correlation between the distance signal of the radar sensor and the laser micrometer can be found. The overall precision is high. Imprecisions occur as the Ellipse fitting could not find an ideal ellipse. This leads to a different amplitude for the radar signal from the reference. For further information please refer to the publication by Gleichauf *et al.*¹. As for us the frequency of the signal is the most important and we showed in Fig. 6 that the frequency is correct and the signals are in sync and in phase, we believe our data is precise enough.

As we showed in our previous publication¹ the dataset was very helpful for developing non-contact respiratory rate detection algorithms. Nonetheless, it has to be said that the here presented neonatal thorax simulator only covers basic functions as for now. In order to simulate more complex breathing patterns as well as the heartrate further development steps would be required.

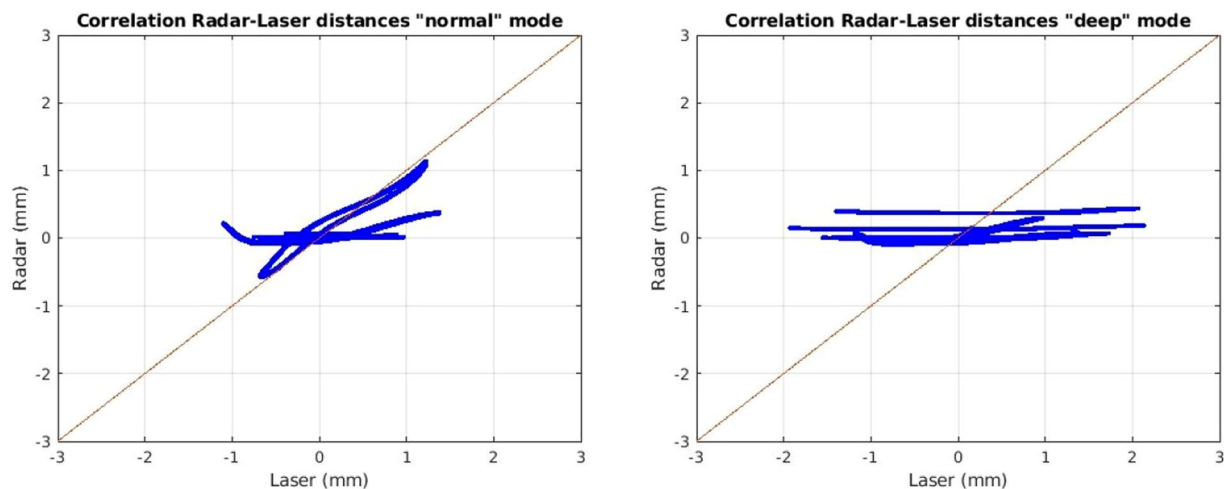


Fig. 8 Correlation between laser and radar distance signal for *normal* (le.) and *deep* (ri.) mode.

| Folder name | Filename | Function |
|-------------|----------------------------|--|
| Radar | iqtocsv.sh | Writes raw IQ-values into csv-file. |
| ToF | pcl_to_png.cpp | Converts ToF pointcloud to png. |
| Laser | convert.m | Calculates Unix timestamps for laser and writes into csv-file. |
| | csv_distance_publisher.cpp | Reads data from csv-file and publishes as ROS-topic. |

Table 4. Overview scripts for generating the dataset.

Usage Notes

The csv-files of the laser and radar data can easily be used and read by i.e. Matlab or any editor. The radar IQ values might be needed to be converted to distance values using the formula above (see Eq. 3). For the ToF data the timestamp has to be read from the png filename first. The depth values (z-value) can easily be written into a pointcloud.

Code availability

Our code for generating the dataset is available within the figshare repository within the scripts folder. An overview over the files can be found within Table 4. For using the laser and ToF C++ code ROS (Kinetic or higher version) needs to be installed. For using the Matlab file (convert.m) a Matlab installation is necessary (i.e. version MATLAB R2022a).

Furthermore the code for generating the signals simulated by the speaker can be found within the scripts folder, too.

Our code may be used under the following terms. The material may not be used for commercial purposes. When using it appropriate credits need to be made. The Creative Commons CC BY-NC 4.0 applies.

Received: 19 October 2023; Accepted: 10 January 2024;

Published online: 23 January 2024

References

- Gleichauf, J. et al. Automated non-contact respiratory rate monitoring of neonates based on synchronous evaluation of a 3d time-of-flight camera and a microwave interferometric radar sensor. *Sensors* **21**, <https://doi.org/10.3390/s21092959> (2021).
- Gleichauf, J., Herrmann, S., Niebler, C. & Koelpin, A. A time-of-flight and radar dataset of a neonatal thorax simulator with synchronized reference sensor signals for respiratory rate detection. *Figshare* <https://doi.org/10.6084/m9.figshare.c.6809370.v1> (2024).

Acknowledgements

The authors thank InnoSenT for providing the interferometric microwave radar sensor. This research was funded by the Federal Ministry of Education and Research (BMBF), Germany (funding reference: 13FH546IX6).

Author contributions

J.G. and S.H. conceived the experiments, J.G. and S.H. conducted the experiments, J.G. and S.H. analysed the results. All authors reviewed the manuscript.

Funding

Open Access funding enabled and organized by Projekt DEAL.

Competing interests

The authors declare no competing interests.

Additional information

Correspondence and requests for materials should be addressed to J.G.

Reprints and permissions information is available at www.nature.com/reprints.

Publisher's note Springer Nature remains neutral with regard to jurisdictional claims in published maps and institutional affiliations.



Open Access This article is licensed under a Creative Commons Attribution 4.0 International License, which permits use, sharing, adaptation, distribution and reproduction in any medium or format, as long as you give appropriate credit to the original author(s) and the source, provide a link to the Creative Commons licence, and indicate if changes were made. The images or other third party material in this article are included in the article's Creative Commons licence, unless indicated otherwise in a credit line to the material. If material is not included in the article's Creative Commons licence and your intended use is not permitted by statutory regulation or exceeds the permitted use, you will need to obtain permission directly from the copyright holder. To view a copy of this licence, visit <http://creativecommons.org/licenses/by/4.0/>.

© The Author(s) 2024